Appendix C

Geostatistical Analysis

This appendix contains a description of the geostatistical analysis performed on the electromagnetic borehole flowmeter (EBF) data contained in Appendix B. This geostatistical analysis was performed to construct alternative conceptual models through stochastic simulation that reflect the heterogeneities observed using the EBF methodology.

Contents

I. Goal of the Geostatistical Study

In a previous study of the Frontier Hard Chrome Site, homogeneous hydrogeologic conductivity distributions were assumed for the contamination zones. Specifically, constant hydrogeologic conductivities were used for the zones. Figure C.1 shows the generalized hydrogeologic conceptual model of the ISRM Pilot Test Site. However, the flowmeter measurements show significant spatial heterogeneity exists in the hydraulic conductivity within each zone. The current geostatistical study aims to build alternative conceptual models reflecting those heterogeneities through stochastic simulation.

The focus of the current study is on the two more permeable zones (A2 and A3) below the most contaminated zone A1. In order to map the conductivity distribution, the absolute conductivity measurements of the borehole are needed. However, the flowmeter experiments only provide information of relative conductivities at depths along the boreholes. Fortunately, average absolute conductivities of the two zones of interest were available from the previous study (see Figure C.1). An overall absolute conductivity of the study zone (joint for A2 and A3 zones) of 6600 was estimated by taking the average of the absolute conductivities of the two zones weighted by the average thicknesses of the zones ([8x1900+5x14000]/13). Because more detailed information is not available, it is further assumed that the average conductivity is constant from borehole to borehole (a strong assumption).

Figure C.1. Generalized Hydrogeologic Conceptual Model of the ISRM Pilot Test Site

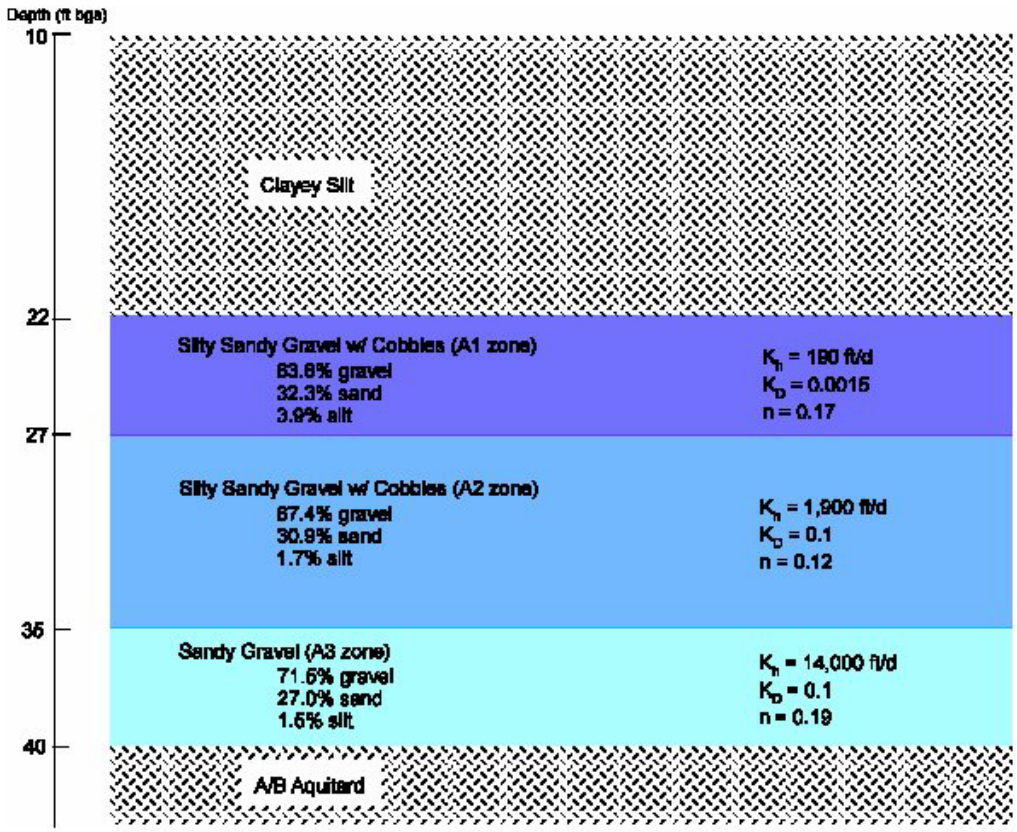

II. Horizontal Coordinate Determination

Flowmeter measurements from eight boreholes were included in the geostatistical analysis and they are PP012, PP016, PP017, PP015, INJ1, PP014 and PP013. Because flowmeter data were not available from PP011, this borehole was excluded from the geostatistical analysis.

The horizontal coordinates for the well were determined based on the ISRM Barrier Installation Plan map shown in Figure C.2. Two sets of coordinates were determined.

X/Y coordinates: The origin of the grid is taken as 3 feet north of PP012.
The axes of the X/Y coordinates are shown in blue in Figure C.2.
Lateral coordinate: The distance between wells; the origin is set to the center of well PP012.

The lateral coordinate is shown in brown arrowed line. In the current study only the heterogeneities of the cross section along the wells were evaluated, so the lateral distance coordinate was used as the horizontal coordinate. The coordinates for each borehole are tabulated in Table C.1.

Figure C.2. ISRM Barrier Installation Plan Map

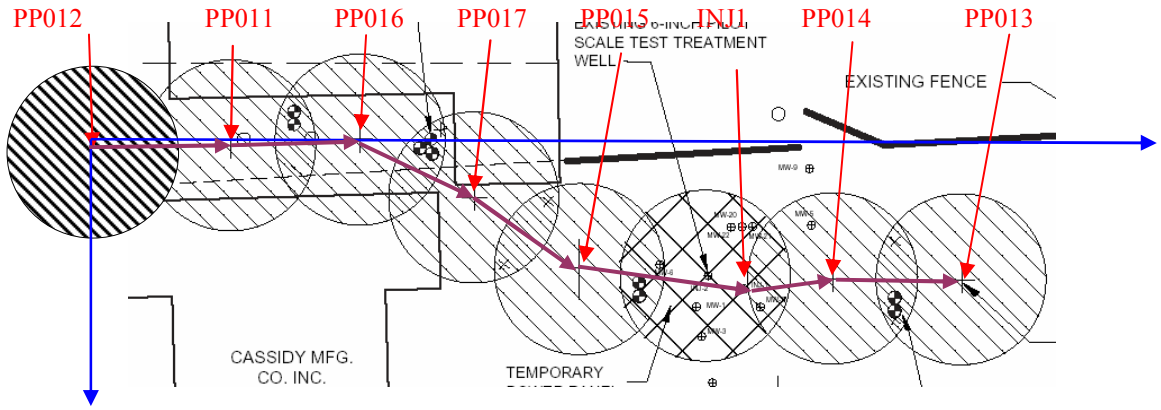

Table C.1. Coordinate determined

		X-Y Coordinates origin: 3 feet north of PP012		Lateral Coordinate origin: PP012		
Borehole No	Borehole Name	X (ft)	Y (ft)	distance	No FM ori	No FM renorm
1	PP012	0	3	0	21	12
2	PP011	35	1.4	35		
3	PP016	65	0	65	22	13
4	PP017	92	13.5	95	21	12
5	PP015	115.5	30	125	21	13
6	INJ1	154	34.5	164	11	7
7	PP014	174.5	32	185	21	15
8	PP013	204.5	32	215	21	15
					137	87

III. Study Domain

Figure C.3 shows the borehole geological profiles. The highest Cr(VI) was observed in the A1 zone (~ between 22 and 27 feet), and the current geostatistical study focuses on the more conductive zones (A2 and A3) below A1 zone (~ between 27 and 40 feet). No stratigraphic coordinate transform was conducted since no severe sinuosity was observed for this short cross section. Instead, a rectangular study domain was used that extended vertically from depths of 25 to 40 ft and extended horizontally 30 ft from each of the two boreholes on both ends of the profile (i.e., PP012 and PP013). A small portion of A1 zone was within the rectangular study domain, therefore a digital boundary separating A2/A3 zones from the A1 zone was determined based on the geological profile shown in Figure C.3. The digital boundary is tabulated in Table C.2. Data falling within the A2/A3 zones were used to evaluate the spatial heterogeneity of the zones and as the conditioning data for simulation. The digital boundary was also used to truncate the simulated cells within the rectangular study area that fall above the boundary with the A1 zone. The study domain of the cross section is shown in blue in Figure C.3. Specifically X0 = -30 ft (30 ft on the left of PP012), X goes along the connecting line between each pair of consecutive boreholes from PP012 to PP013 and extends to Xmax = 245 ft, 30 ft to the right of PP013. Y0 = 25 ft, and Y goes from top to bottom of the boreholes with Ymax = 40 ft.

Table C.2. Boundary of the study domain

Borehole	PP012	PP016	PP017	PP015	INJ1	PP014	PP013
Bottom	38.00	38.00	39.00	40.00	40.00	40.00	40.00
Top	27.00	27.00	27.00	27.00	27.00	26.00	25.00

Figure C.3. Geological profiles of boreholes

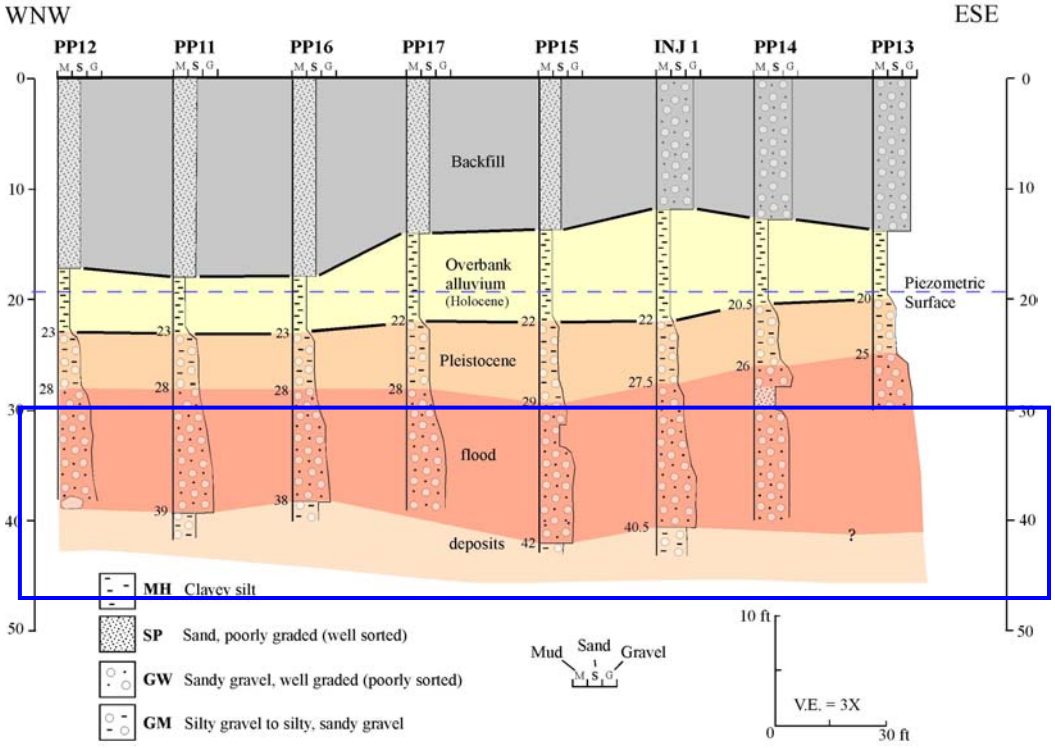

IV. Data Renormalization and Calibration

The flowmeter data were originally reported as relative conductivities normalized to unity for each borehole. The borehole profiles of the relative conductivity are shown in Figure C.4. Because the current spatial analysis focuses only on the two lower zones of the formation, data above these two zones were truncated and only flowmeter data in the two zones were kept and re-normalized to unity. The borehole profiles of the renormalized relative conductivity are shown in Figure C.5. The relative conductivities of the boreholes were then calibrated to the average absolute conductivity estimate of 6600 ft/d, and estimations of absolute conductivities were obtained. Figure C.6 shows the borehole profiles of the estimated absolute conductivities. Figure C.7 shows the histogram of the estimated absolute conductivities of all boreholes together. The data were transformed to normal scores for evaluation of the spatial heterogeneity via variogram analysis and for the sequential Gaussian simulation.

Figure C.4. Borehole Profiles of Relative Conductivity

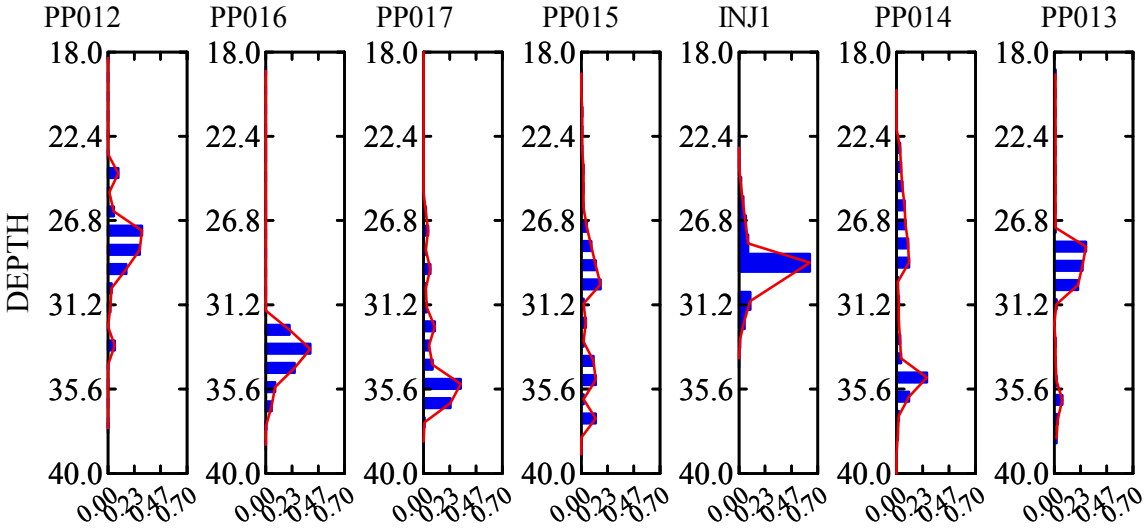

Figure C.5. Borehole Profiles of Truncated and Renormalized Relative Conductivity

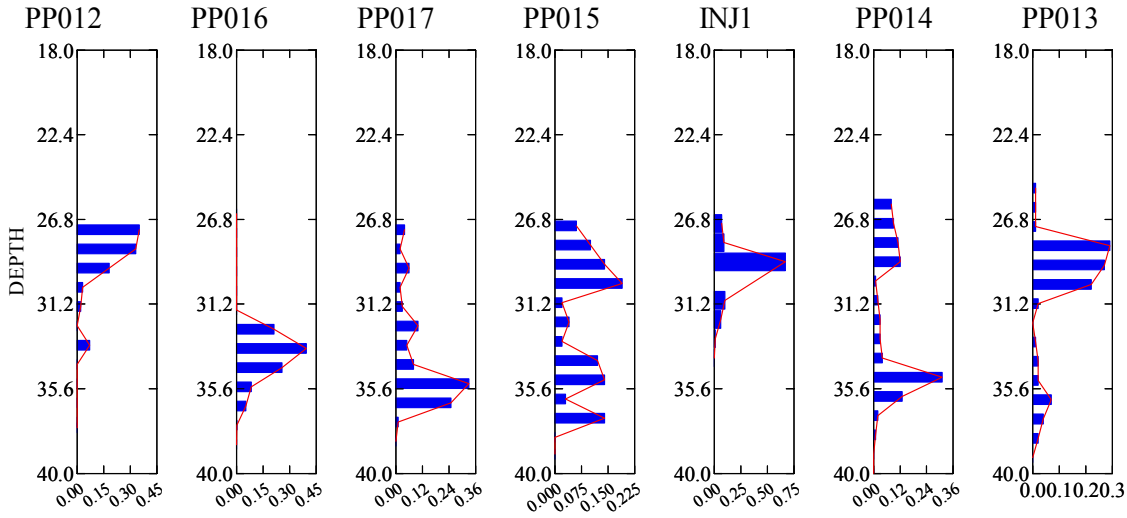

Figure C.6. Borehole Profiles of Estimated Absolute Conductivity

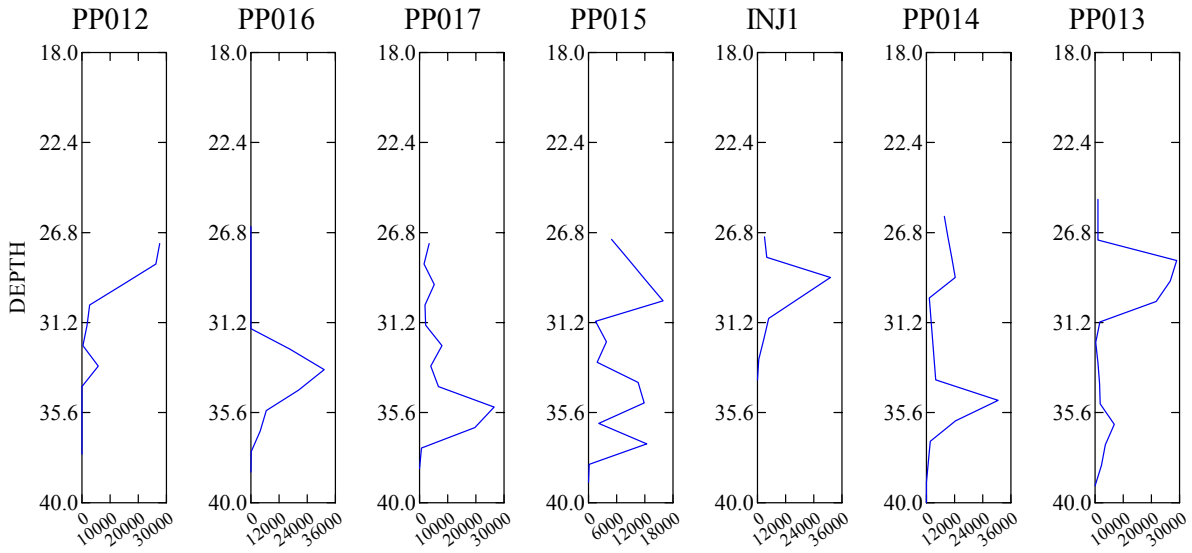

Figure C.7. Histogram of the Estimated Absolute Conductivity

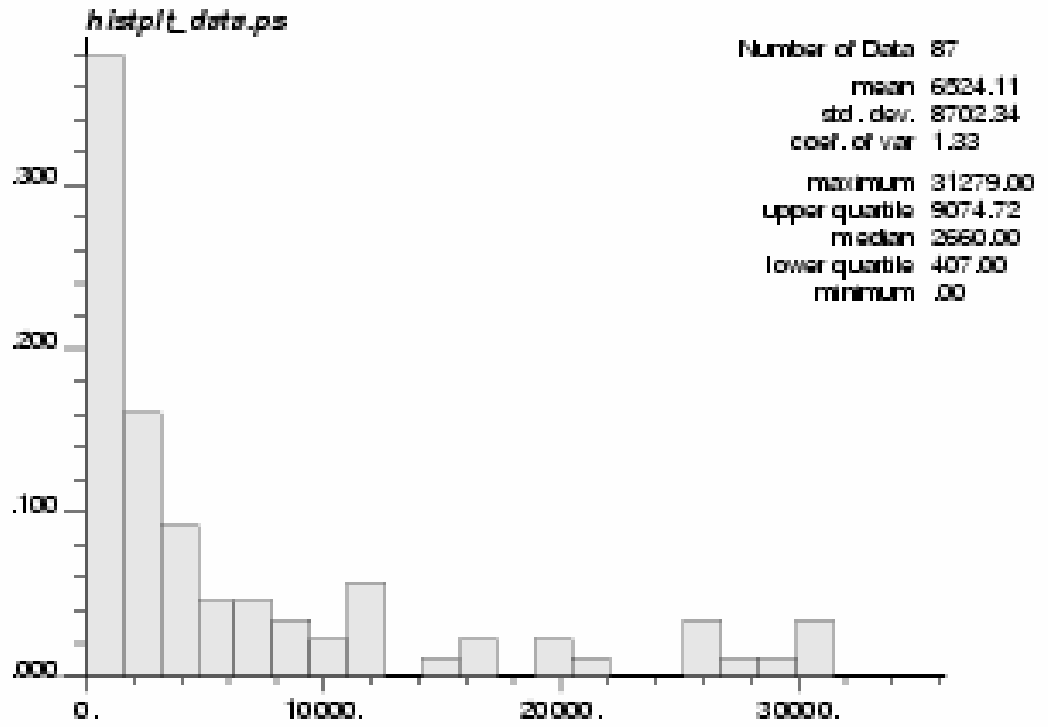

V. Variogram Analysis

Vertical and horizontal variograms were calculated for the normal score transformed data. There were enough data for inferring a vertical variogram model but a reliable horizontal (lateral) variogram model could not be derived from the seven boreholes. Figure C.8 shows the experimental variograms and the variogram models fitted. The fitted variogram model is shown in the equation below Figure C.8.

Figure C.8. Nscore Variograms and Models

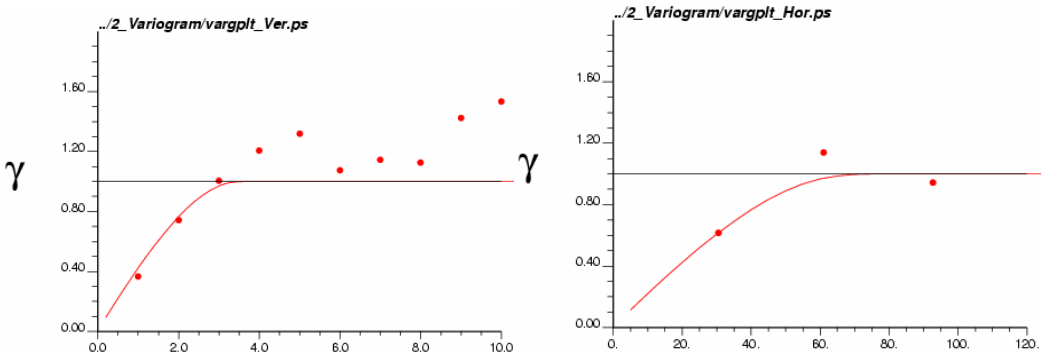

$$\gamma = 0.01 + 0.49 \times Sph\begin{pmatrix}3.5\\65\end{pmatrix} + 0.50 \times Sph\begin{pmatrix}3.5\\75\end{pmatrix}$$

VI. Simulation

The variogram models were used as input for the sequential Gaussian simulation. The simulation resolution was defined as 1 foot horizontally and 0.5 feet vertically. Each simulation realization consists of 8556 (216 by 31) points and a total of 101 realizations were generated. Figure C.9 shows two realizations as examples. Figure C.10 shows the map of the mean values of the hydraulic conductivity derived by averaging the values at each grid node for the 101 realizations. It should be noted that the X/Y ratio of the images is intentionally distorted to allow better visualization.

Figure C.9. Two Realizations

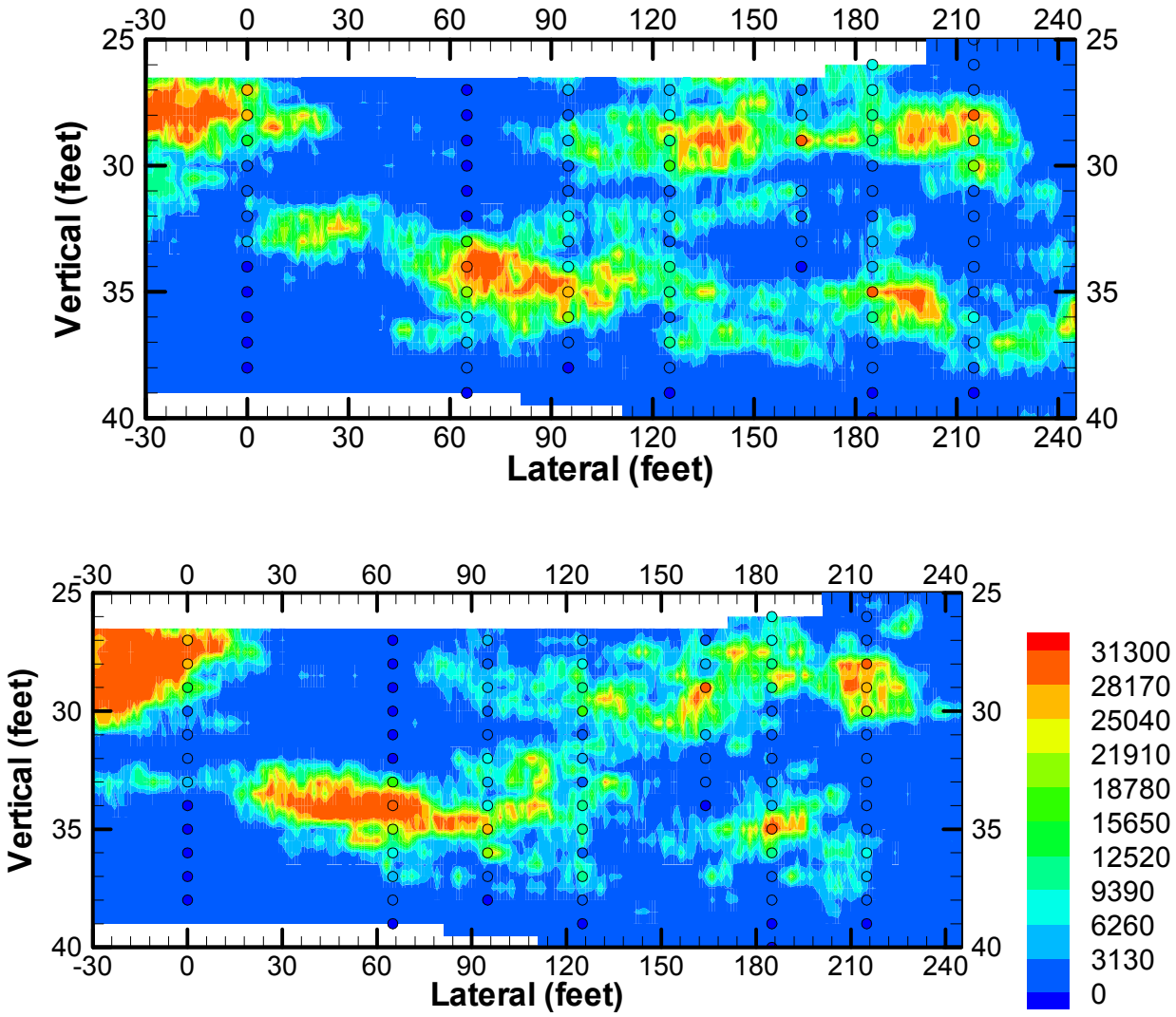

Figure C.10. E-Type Map

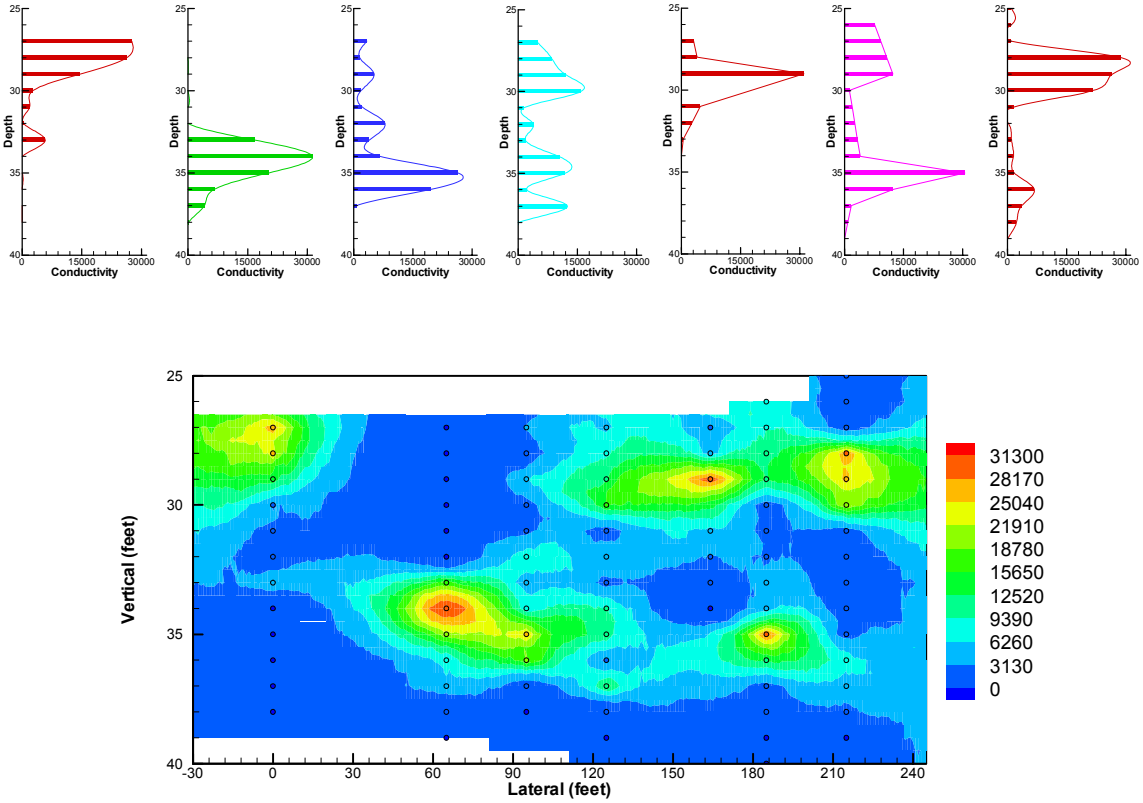

Figure C.11. Histograms of Two Individual Realizations

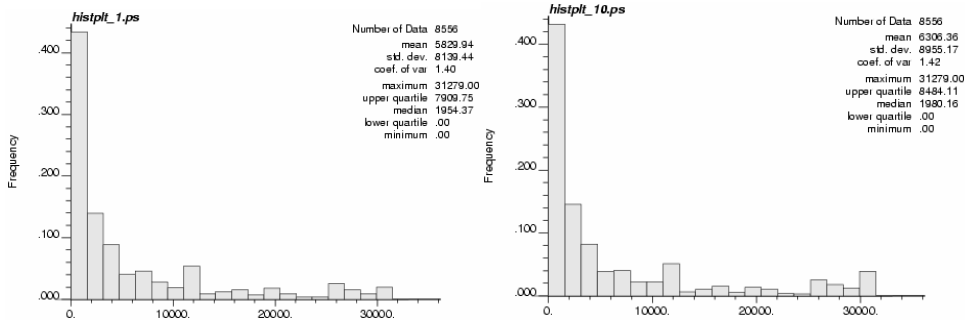

Figure C.12. Variograms of 11 Individual Realizations (Red) and Variogram Model (Blue). Horizontal (Left) and Vertical (Right)

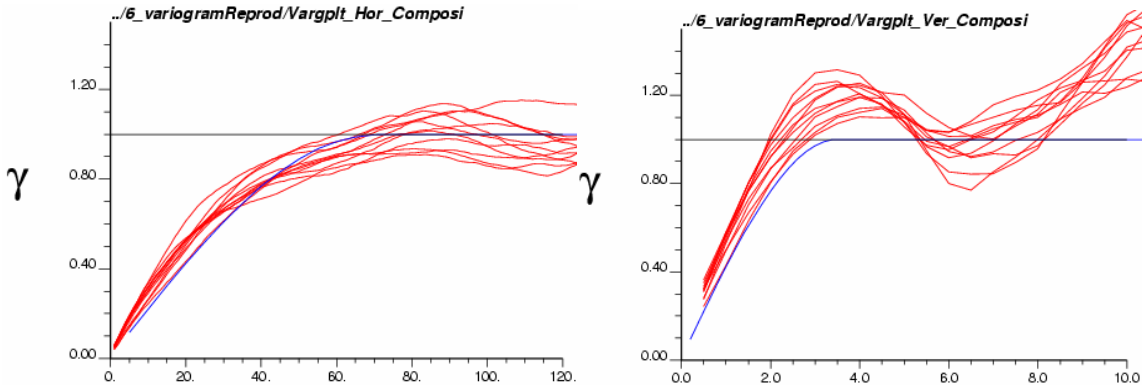

VII. Post-Processing of Simulations

The simulated hydrological conductivity field will be used in numerical models to evaluate the flow and transport behavior. All simulated realizations are equally probable scenarios of the hydrological conductivity, but each realization will result in slightly different flow and transport behavior. Processing the suite of all realizations in the numerical flow and transport model would allow assessment of the uncertainty in the flow behavior. However, it is computationally impractical to process all the individual realizations through the numerical flow model. One possibility is to use the E-type model presented in Figure C.10 as the most probable representative of the hydraulic conductivity present at each node. However, the E-type estimate, like those obtained from other interpolation methods like kriging or fitting splines to the data, tends to be a smooth representation. Unlike the individual realizations, it does not capture the full spatial variability observed in the data. In order to run a limited number of realizations that would provide information on the variability that might be expected in flow and transport, it is beneficial and computationally feasible to rank the realizations and then use several realizations that sample the extremes of the ranking for the flow and transport modeling.

A ranking procedure was developed for this study based on a modification of Clayton Deutsch's published method for generating geo-objects and ranking individual realizations. Geo-objects are defined for each conductivity realization. A set of connected cells with conductivity larger than a predefined threshold forms a geo-object. Multiple geo-objects can be formed for each conductivity realization. For the injection experiment at the Frontier Site, only geo-objects that intersect the injection wells are important. Therefore, both the location of the injection wells and the distribution of the geo-objects in a realization determine the transport behavior of the realization. Deutsch's original programs of geo_obj and rank_loc enable the calculation of geo- objects and the cumulative number of net cells (those that exceed the conductivity threshold). Realizations are thus able to be ranked in terms of the cumulative number of net cells in the realizations. Considering the skewed distribution of the conductivity seen in this study, the conductivities in the net cells could be very different and the cumulative number of net cells alone might not be a good criterion for the ranking. Instead, the cumulative conductivity of the net cells that intersect an injection well was used as the ranking criterion.

The following ranking procedure was developed:

1. Calculate the geo-objects for each realization using a conductivity value of 2660 ft/d as a cutoff for identifying net cells.
2. Evaluate each of the six wells serves as the injection well. A 15 feet search radius is used to cumulate the net cells intersected with the injection well and a cumulative conductivity is calculated for the injection well.
3. Realizations are ranked according to the cumulative conductivity for each potential injection well.

Table C.3 lists the ranking results. For each injection well, the realization index of the two most conductible, the least conductible and the one with medium conductivity are listed in Table C.3 together with the cumulative conductivity values. The corresponding conductivity maps around each injection well are shown in Figure C.13.

Table C.3. Ranking results

	PP011		PP012		PP013		PP014	
Rank			real	cumuCond	real	cumuCond	real	cumuCond
1st most perm	45	6494340	15	5580115	57	7175821	61	7778516
2nd most perm	65	5180520	18	5526106	11	6942426	22	7611468
middle	73	2090579	32	4113719	52	5355820	91	5615368
2nd least perm	17	6470	101	2457202	4	3738044	96	4060863
1st least perm	10	0	62	2419862	43	3693845	54	3891228

	INJ1		PP015		PP016		PP017	
Rank			real	cumuCond	real	cumuCond	real	cumuCond
1st most perm	38	8646478	43	7544471	81	5652942	94	5913057
2nd most perm	19	8132086	11	7514036	27	5553519	11	5840530
middle	13	5076646	88	5278941	76	4336754	40	4525658
2nd least perm	70	3666572	45	3384502	79	3297546	88	3358777
1st least perm	35	3616893	62	3334711	20	3266344	9	30001492

Figure C.13. Conductivity Maps Around Each Potential Injection Well of the Five Selected Realizations Listed in Table C.3 and the Mean of all 101 Realizations (the last one)

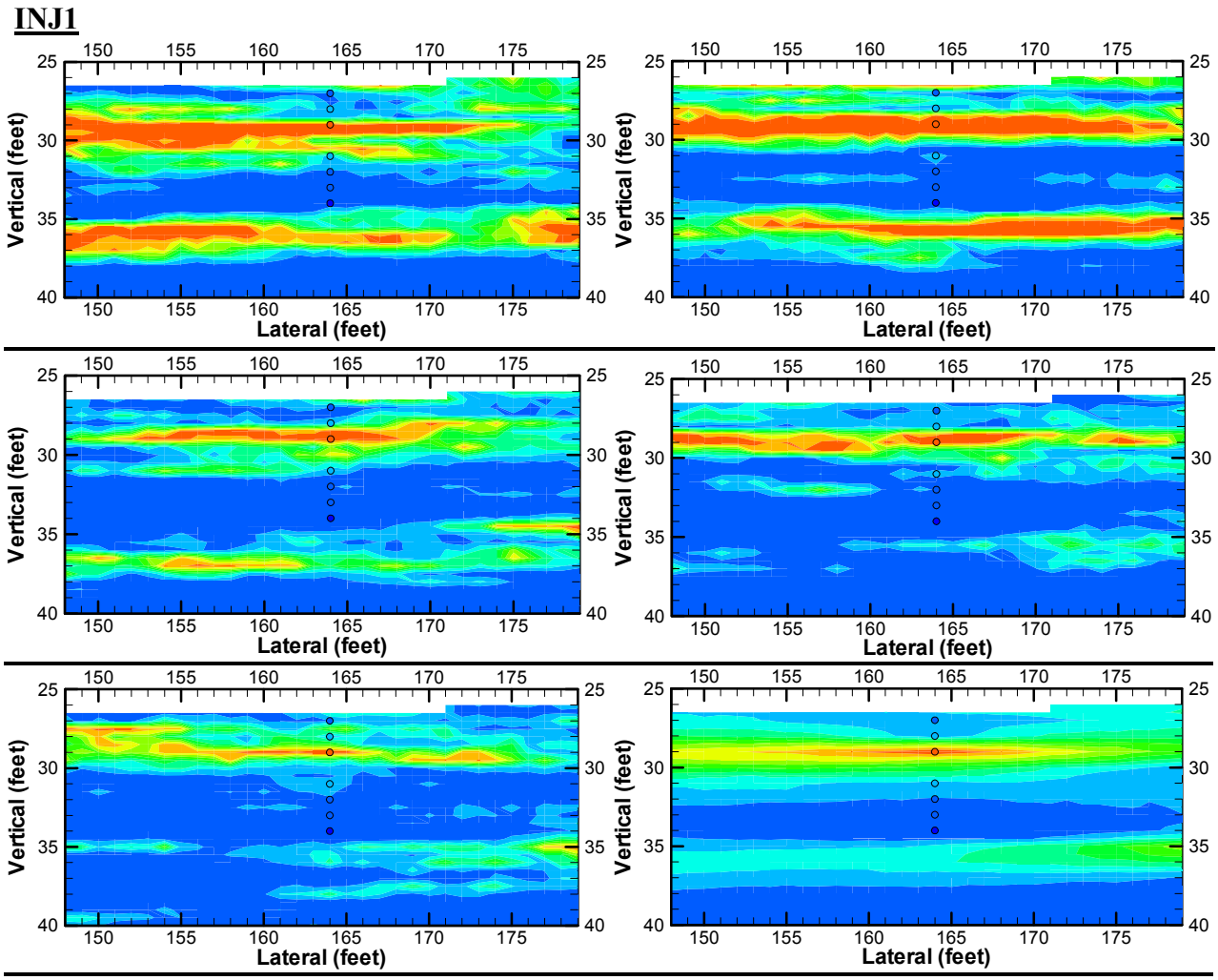

PP011

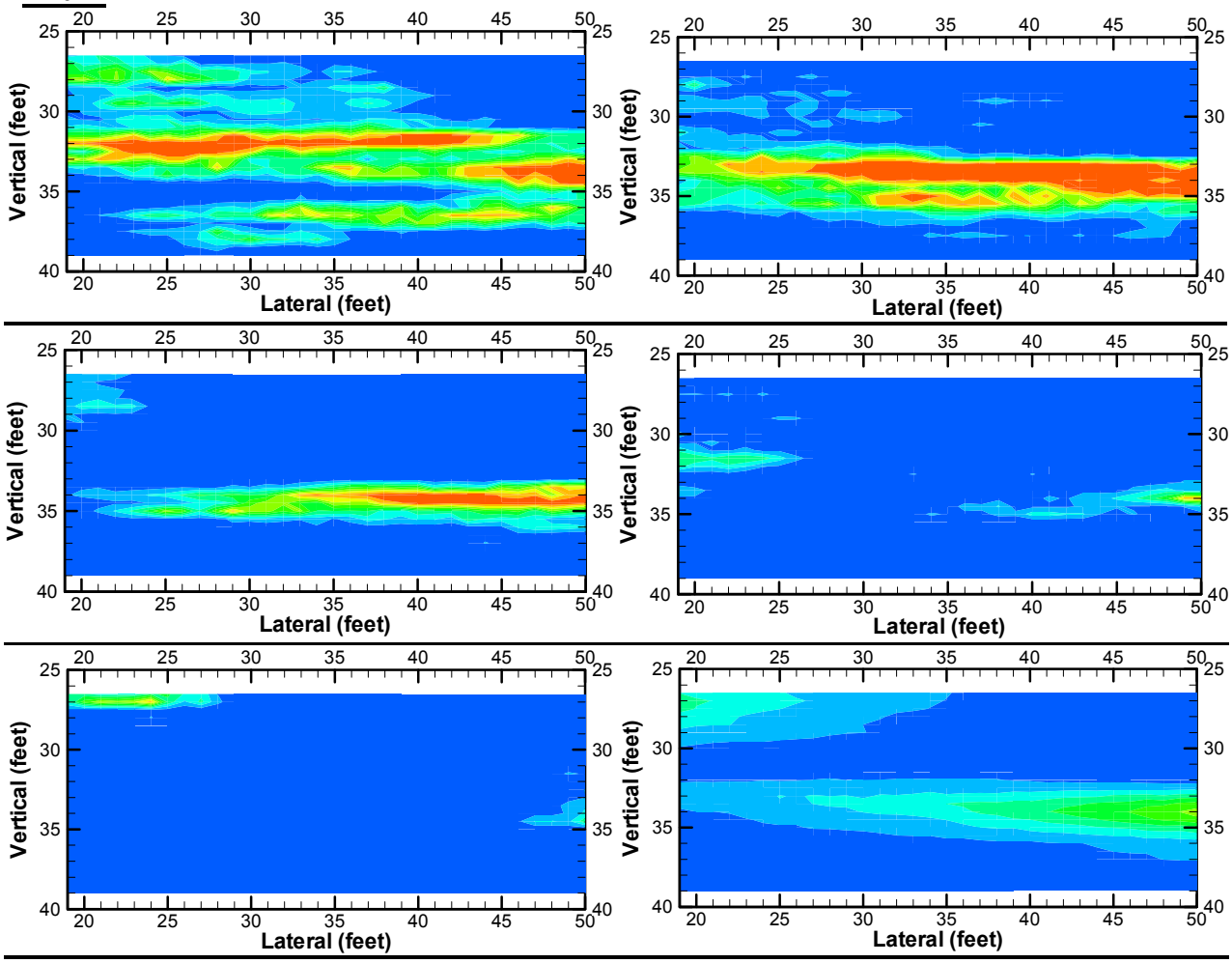

PP012

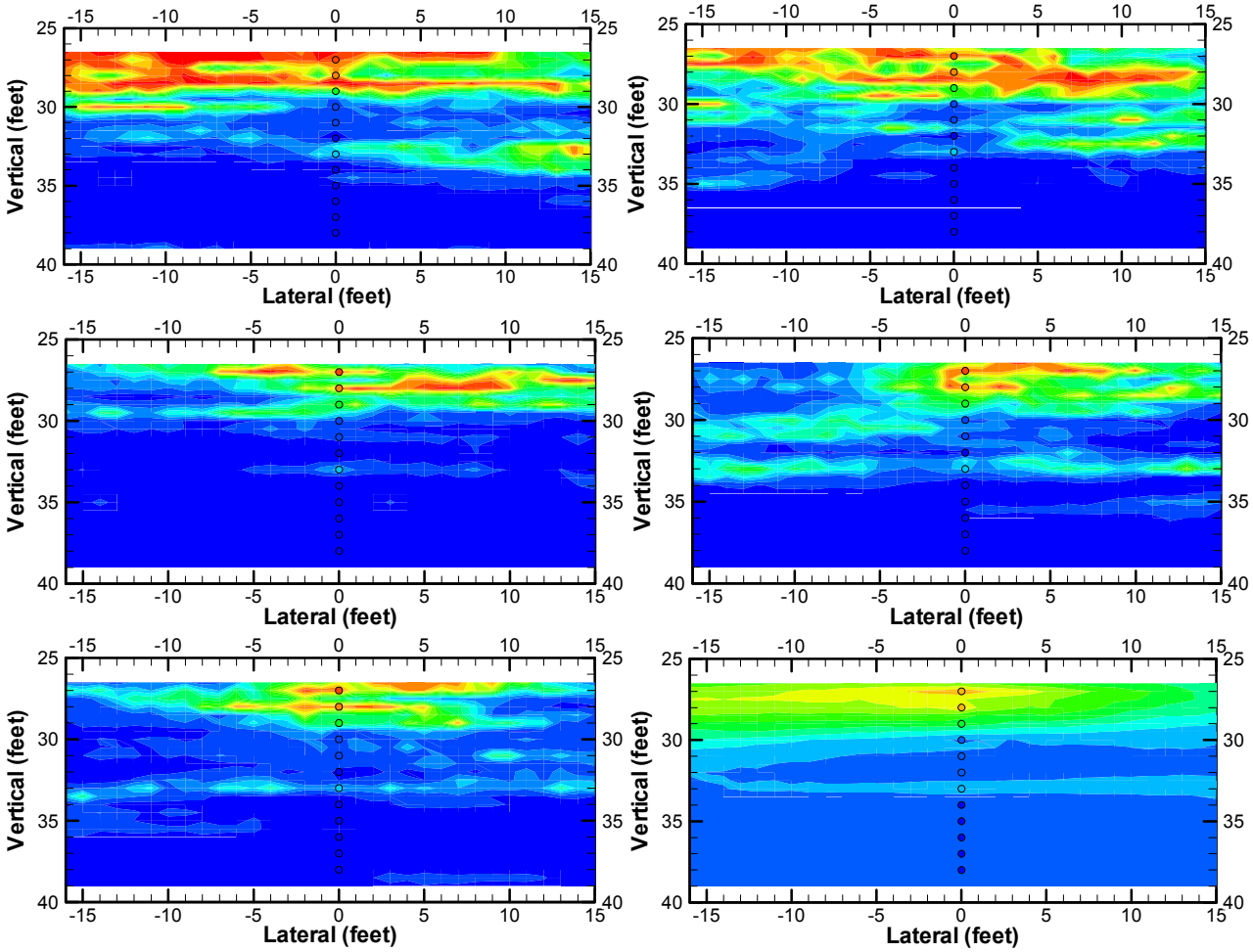

PP013

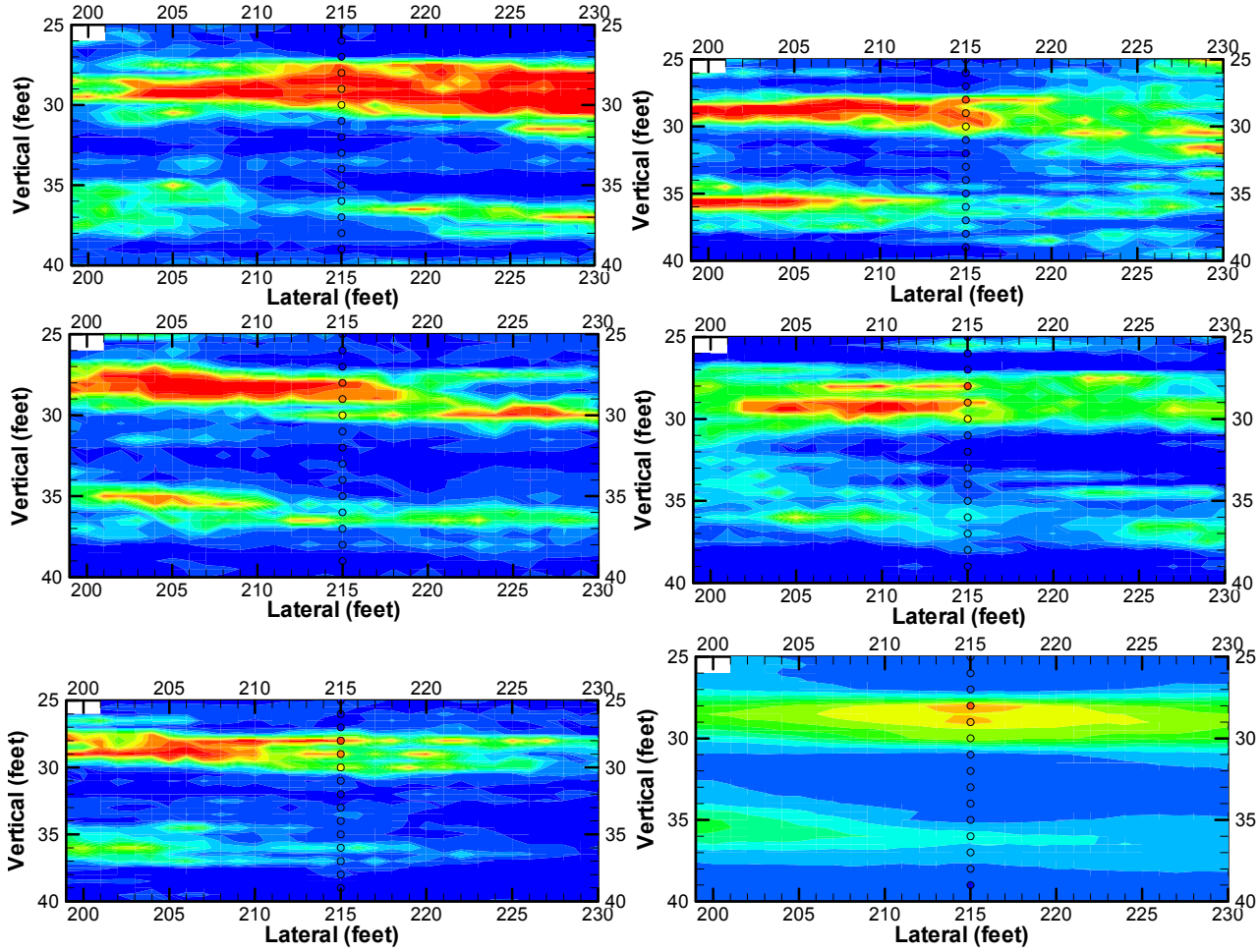
Vertical (feet)
Lateral (feet)
200
205
210
215
220
225
230
25
30
35
40

PP014

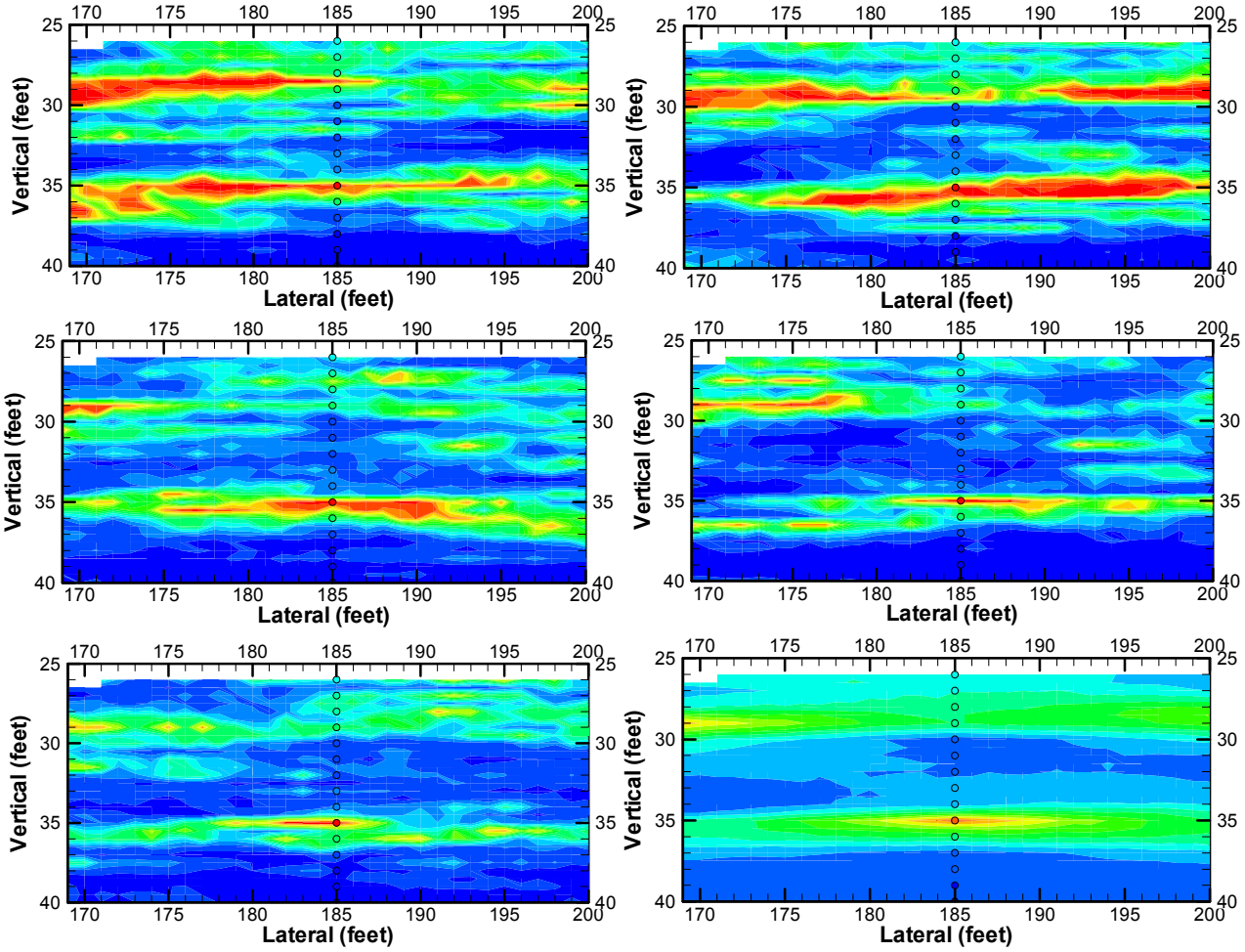
Vertical (feet)
Lateral (feet)
25
30
35
40
170
175
180
185
190
195
200

PP015

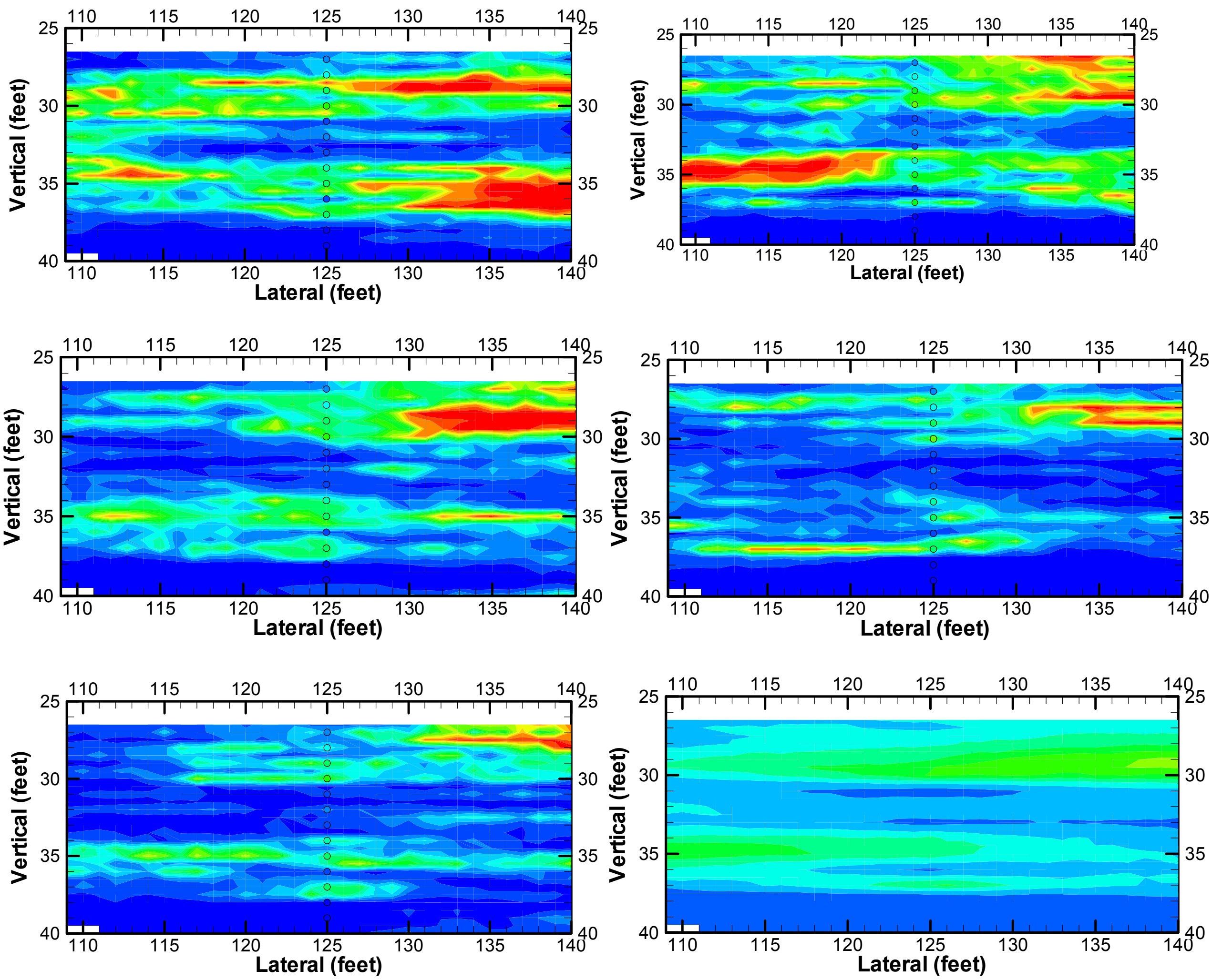
Vertical (feet)
Lateral (feet)
110
115
120
125
130
135
140
25
30
35
40

PP016

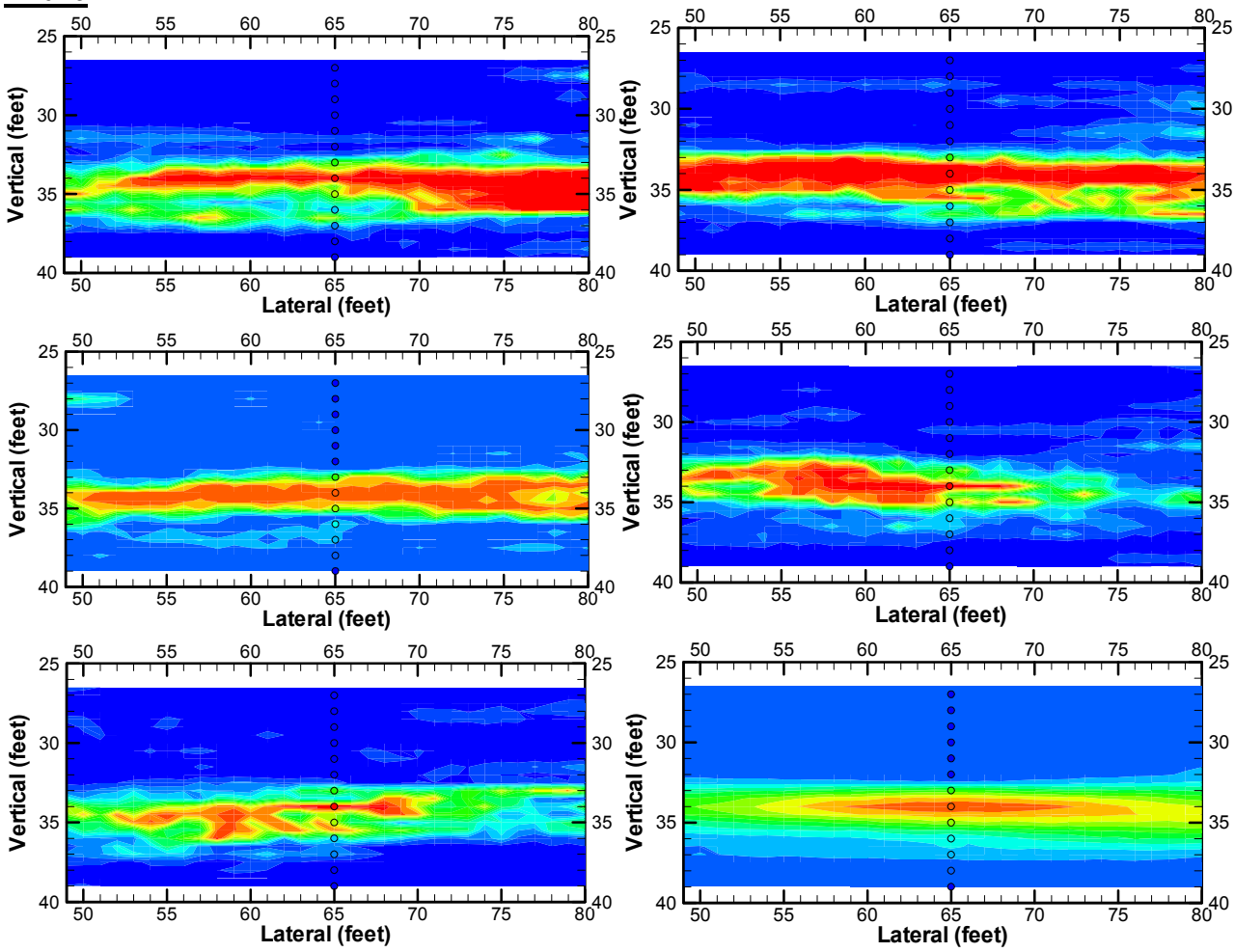

PP017

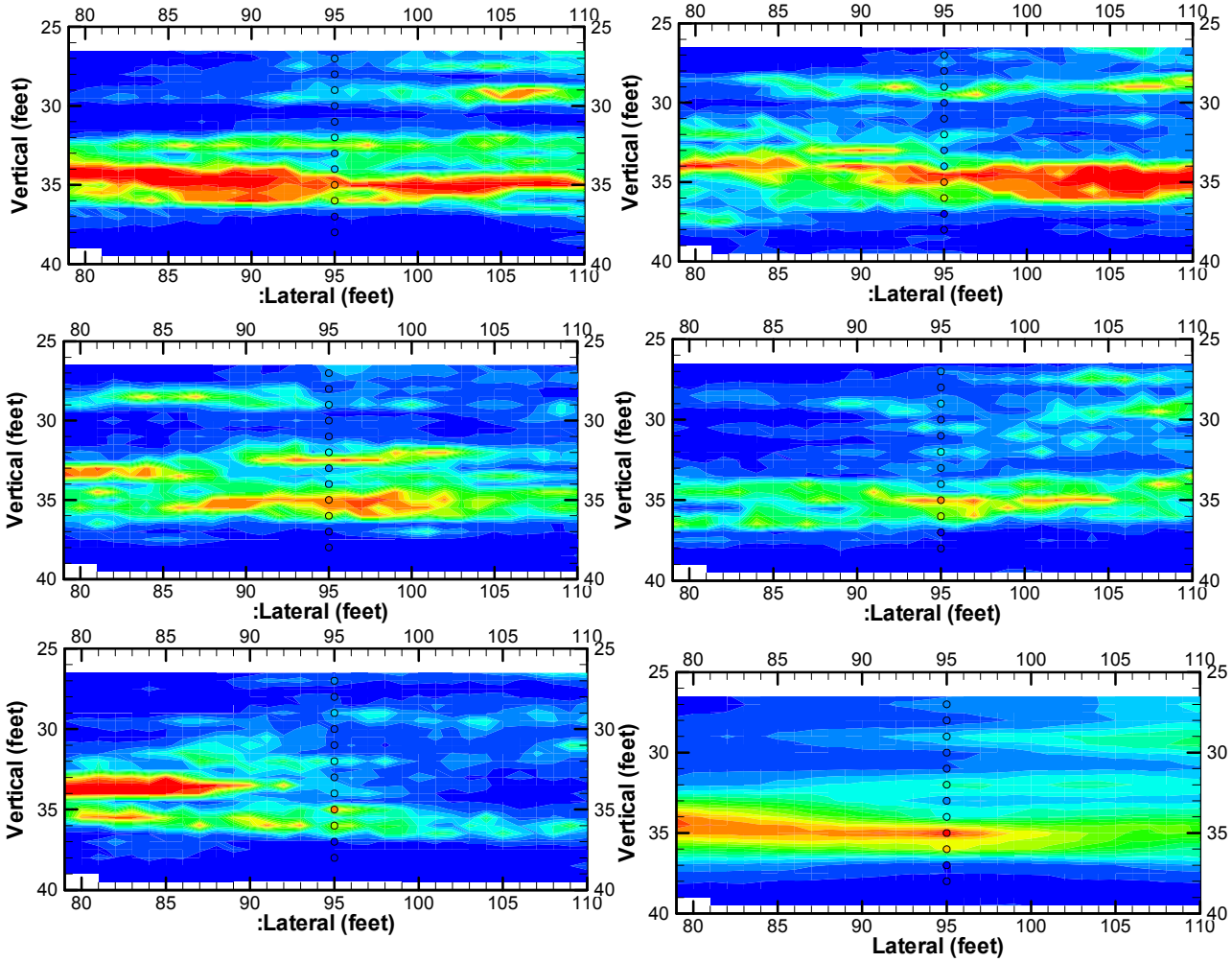
Vertical (feet)
:Lateral (feet)
Lateral (feet)
80
85
90
95
100
105
110
25
30
35
40